

RESEARCH MEMORANDUM

SOME EFFECTS OF ROUGHNESS ON STAGNATION-POINT HEAT
TRANSFER AT A MACH NUMBER OF 2, A STAGNATION
TEMPERATURE OF 3,530° F, AND A REYNOLDS
NUMBER OF 2.5×10^6 PER FOOT

By H. Kurt Strass and Thomas W. Tyner

Langley Aeronautical Laboratory
Langley Field, Va.

LIBRARY COPY

MAY 26 1958

LANGLEY AERONAUTICAL LABORATORY
LIBRARY, NACA
LANGLEY FIELD, VIRGINIA

CLASSIFIED DOCUMENT

This material contains information affecting the National Defense of the United States within the meaning of the espionage laws, Title 18, U.S.C., Secs. 793 and 794, the transmission or revelation of which in any manner to an unauthorized person is prohibited by law.

NATIONAL ADVISORY COMMITTEE FOR AERONAUTICS

WASHINGTON

May 26, 1958

~~CONFIDENTIAL~~



3 1176 01437 7908

NATIONAL ADVISORY COMMITTEE FOR AERONAUTICS

RESEARCH MEMORANDUM

SOME EFFECTS OF ROUGHNESS ON STAGNATION-POINT HEAT

TRANSFER AT A MACH NUMBER OF 2, A STAGNATION

TEMPERATURE OF $3,530^{\circ}$ F, AND A REYNOLDSNUMBER OF 2.5×10^6 PER FOOT


By H. Kurt Strass and Thomas W. Tyner

SUMMARY

A limited investigation has been conducted to determine some effects of surface roughness on heat transfer at the stagnation point. The tests were made in the ceramic-heated jet (laboratory model) at a Mach number of 2, a stagnation temperature of $3,530^{\circ}$ F, and a stream Reynolds number of 2.5×10^6 per foot. The results are given as functions of the root-mean-square roughness, roughness Reynolds number, and macroscopic surface area increase. These data show little effect of surface roughness upon the heat transfer for roughness values below approximately 40 microinches. In the roughness range greater than 40 microinches, the heat transfer was shown to be a function of the surface roughness and roughness Reynolds number. At very large values of surface roughness (equal to, or larger than, the displacement thickness of the boundary layer at the stagnation point) the data tend to show that the heat transfer is dependent upon the macroscopic surface area.

INTRODUCTION

Some recent preliminary experiments have indicated that the heat transfer to the face of a bluff body is markedly affected by the detail shape of the surface. Firing tests from a high-velocity gun at approximately 6,000 ft/sec have shown that shallow grooves in the face of flat-face magnesium projectiles are sufficient to cause burning of the projectiles, whereas unmarked projectiles showed no evidence of burning. Similar tests made in the ceramic-heated jet (laboratory model) at a Mach number of 2 and stagnation temperature equal to approximately $3,500^{\circ}$ F showed that the time to melt of flat-face steel specimens was



decreased when the surface area was increased by machining grooves into the face.

In order to examine more closely the relationship between the surface characteristics and the heating rate of flat-face bodies, a series of tests were made in the ceramic-heated jet (laboratory model) of 10 flat-face models with surface roughnesses varying from about 7 micro-inches rms to macroscopic values. (See table I.) These tests were conducted at a Mach number of 2 and a stagnation temperature equal to approximately 3,530° F. Detailed test conditions are given in table II.

SYMBOLS

c_p	specific heat of Inconel, Btu/lb-°F
h	heat-transfer coefficient, Btu/(sq ft)(sec)(°F)
T	temperature, °F
t	time after start of test, sec
ω	ratio of model weight to projected area, lb/sq ft

Subscripts:

stag	stagnation-point conditions
B	rear surface
F	front surface

MODELS AND TESTS

General Description

The test models were 3/4-inch-diameter Inconel disks with a nominal thickness of 1/16 inch before surface preparation. The outer surface of each model was subjected to a different treatment so that the range of surface roughness varied from about 8 to 13,700 microinches. All models were instrumented with three chromel-alumel thermocouples welded to the back face of the disks as shown in figure 1. The models were cemented to molded aluminum oxide insulating supports with Sauereisen 76 cement. Contact area between the model and support was limited to the outer edge

by a tapered clearance hole through the support; errors resulting from heat loss to the support were thus minimized. A typical model, its insulating support, and test sting are shown in figure 2.

The individual model surfaces are described in table I and by means of photographs and sketches in figures 3 to 12. Figure 3 shows all the models which, with the exception of models 4 and 5, are numbered in order of decreasing surface roughness, the values of which are presented in table I.

All the models were tested in the ceramic-heated jet (laboratory model) at a Mach number of 2, a stagnation temperature of approximately $3,530^{\circ}\text{F}$, a stream Reynolds number of 2.5×10^6 per foot, and a jet diameter of 1 inch. During all tests, the models were approximately 0.25 inch downstream from the nozzle. Reference 1 gives a complete description of the jet and its operation.

Model measurement.- Measurements of surface roughness and area were obtained in several ways inasmuch as no one method was applicable to the range of roughness studied here. This procedure also gave a check on the various methods where their regimes of applicability overlapped.

In the case of models 1, 2, and 3, the measurements were made optically by using conventional techniques with an accuracy of about ± 0.001 inch. These measurements were limited to the macroscopic detail on the assumption that heating effects attributable to the overall pattern of microscopic detail were negligible in comparison with those caused by the macroscopic detail.

Roughness measurements on models 4 to 8 were made by using the Physicists Research Co. Profilometer, Model No. 11, Type Q, which gives average roughness values in microinches rms. In addition, roughness values were obtained by sectioning duplicate models and taking the necessary measurements from the photomicrographs of the cross sections which are reproduced in figure 12. The models were prepared for sectioning by plating a thin layer of copper upon the surface on top of which was plated a thicker layer of nickel. The dark line shown in the photomicrographs reproduced in figure 12 is the copper plating and each picture is arranged in such a manner that the area immediately below this line is the model material and the area above the line is the nickel plating. The true surface of the model then exists at the lower edge of the dark line. Maximum accuracy of measurement was obtained by making the measurements from 10-diameter enlargements made from the glass photomicrograph negatives. Surface irregularities as small as 1 microinch could be detected by this method. The cross sections were polished and photomicrographed by conventional methods.

The root-mean-square value of roughness is the standard parameter used in denoting the quality of surface finishes. This method gives a special average of heights above and below a mean surface. It tends to emphasize the higher peaks since a series of high narrow peaks would have little effect on positioning the mean line but would greatly influence the surface quality. A more detailed discussion of these effects may be found in references 2 and 3.

The increase in surface area attendant with increased roughness was approximated by measuring the actual length of line of the interface separating the copper plating and the surface and dividing by the straight-line distance between the end points of the measurement. It was assumed that, since the surfaces of models 4 to 8 were prepared by processes involving the unidirectional removal of material, the surface area was then proportional to the length of line of the interface. Models 9 and 10 were measured with a surface interferometer (Type L.C.A., No. 36) manufactured by La Précision Mécanique (Paris). Numerous readings were taken in the vicinity of the stagnation point in order to get a fairly representative value. Duplicates of models 9 and 10 were also sectioned and measured by means of photomicrographs. The single section through the stagnation point of these models did not provide sufficient information to establish any relationship between the linear measure along the interface and the surface area inasmuch as models 9 and 10 were hand polished and the resulting surface was probably random in nature. The relative increases in lineal measure of the interfaces to the projected lengths are included in table I purely as a matter of interest inasmuch as little significance is attached to these values.

Heat-transfer calculations.- Figure 13 presents a typical example of the variation with time of the rear-surface temperature at the stagnation point. For comparison, the estimated variation with time of the front-surface temperature as calculated by the methods of references 4 and 5 are also shown. Reference 4 was used to define the curve near the origin where the method of reference 5 was least accurate. A maximum difference of approximately 360° F between the front and rear surfaces was indicated by these methods.

Figure 14 shows temperature variations normal to the longitudinal center line of the models at the stagnation point and at 0.05 and 0.1 inch radially from the center. During the tests, three thermocouples proved defective and no data are available for these points. The data for this figure were taken at 0.5 second after time zero for which time the heat-transfer calculations were made. These temperature gradients were very small and were neglected in the determination of the heat-transfer coefficients at the stagnation point.

The heat-transfer coefficients were determined in the first 3/4 second of the test in order to minimize conduction errors and changes in the character of the surfaces resulting from the impact of minute particles of zirconia which are carried by the airstream. These particles are generated by thermal action in the bed of zirconia balls which provide the reservoir of heat for the operation of the hot jet (ref. 1). The frequency of impact of these particles has not been determined but it is sufficiently low to assume with reasonable assurance that the measured heat-transfer coefficients are representative of the original surfaces. Radiation interchanges between the model and the heated pebble bed and between the model and the surrounding air were negligible at the low temperatures at which these data were evaluated. Neglect of radiation losses and temperature gradients normal to the center line of the models permits the calculation of the heat-transfer coefficients by means of the following approximate expression:

$$h = \frac{c_p \omega}{T_{stag} - T_F} \frac{dT_B}{dt}$$

The slope dT_B/dt was measured over a one-half second of time centered about $t = 0.5$. At this time, the temperature gradients normal to the model surface were essentially invariant with time as evidenced by the example of figure 13 where it is seen that the slope of the calculated front-surface temperature is approximately the same as that measured for the rear surface at this time and no gradient correction is needed.

RESULTS AND DISCUSSION

Figure 15 presents the variation of the stagnation-point heat-transfer coefficient with surface roughness. As a matter of interest, the theoretical value computed by the method of reference 6 with the velocity gradient at the stagnation point computed from reference 7 is also shown. The minimum measured heat-transfer coefficient is about 25 percent greater than the theoretical value. Comparisons of some unpublished data with values calculated by theory have shown good agreement. The reason for the relatively large experimental minimum heat transfer measured in these tests as compared with values calculated by the theory of reference 6 is not known at this time. With the experimental accuracy of the technique, no systematic effect of changing the surface roughness is observable in the roughness range from 0 to approximately 40 microinches rms. However, in the roughness range greater than 40 microinches, there is a trend of increased heat transfer with increased

roughness. Heating rates up to 75 percent greater than the minimum values were measured with the roughest surfaces.

Somewhat similar results are presented in reference 8 for the heat transfer at the stagnation point of a hemisphere. Two values of roughness were tested over a range of wind-tunnel operating conditions. The results were correlated as a function of the roughness Reynolds number and also show a region of little or no effect of the roughness Reynolds number for low values of this parameter. Roughness Reynolds number is defined as the product of free-stream Reynolds number per foot and the root-mean-square roughness. A definite trend of increasing heat transfer with increased values of roughness Reynolds number is shown to exist after this initial invariant zone.

The data from the present tests were normalized in terms of the minimum measured heat transfer (model 8) and the results were plotted as a function of roughness Reynolds number in figure 16. The data of reference 8 are also included in this figure for purposes of comparison. The data of reference 8 seem to indicate a greater increase in heat transfer with increasing roughness Reynolds number than do the results of the present tests.

The heat-transfer coefficient for model 4 seems unusually low when compared with the value for model 6 which was only slightly rougher but experienced a much higher heating rate. Little significance is attached to the fact that the calculated roughness for model 4 is quite different from the profilometer value (see table I) since a rough ground surface is inherently subject to great variation when considered on a microscopic scale, as may be seen from examination of the photomicrographs of the surface presented in figure 12. This difference is believed to be the result of inadequate sampling by the photomicrographic technique. It is apparent from examination of the data of models 1, 2, and 3 that some surface parameter other than mean roughness must affect the stagnation heat transfer. These models experienced widely different heating rates but, according to the method of measurement, had about the same surface roughness. Replotting these data as in figure 17 implies that the heating rate was a function of the macroscopic area increase. The mean surface roughness of these models was approximately 13 times the stagnation-point displacement thickness of the boundary layer. This thickness was calculated to be on the order of 0.001 inch by the subsonic, incompressible, two-dimensional relationship given in reference 9. Model 5 (rough machined surface) had a measured microscopic area increase of 30.9 percent over the projected area or very nearly the same as the macroscopic area increase of model 3 (unidirectional grooves), but showed much less heating. The mean surface roughness as calculated from the photomicrographs (model 5) was of the same order of magnitude as the calculated displacement thickness of the boundary layer and also the same order as the lower limit of

macroscopic measurement. On a macroscopic scale, very little surface protrusion through the boundary layer must have occurred. Likewise, the macroscopic area increase must have been very small. Thus, in these tests, the macroscopic area increase becomes also a measure of the surface area which protrudes through the boundary layer and suggests an explanation for the relatively lower heating rate for model 5 as compared with model 3.

CONCLUDING REMARKS

The results of these tests indicate that the heat transfer at the stagnation point varies considerably with the condition of the surface at this point. Little effect of roughness upon the stagnation-point heat transfer was observed for roughness values below approximately 40 microinches. For values of roughness larger than 40 microinches, the heat transfer was shown to be a function of the surface roughness. At very large values of surface roughness, the data tend to show that the heat transfer is dependent upon the macroscopic surface area.

Langley Aeronautical Laboratory,
National Advisory Committee for Aeronautics,
Langley Field, Va., February 21, 1958.

REFERENCES

1. Fields, E. M., Hopko, Russell N., Swain, Robert L., and Trout, Otto F., Jr.: Behavior of Some Materials and Shapes in Supersonic Free Jets at Stagnation Temperatures Up to 4,210° F, and Descriptions of Jets. NACA RM L57K26, 1958.
2. Spotts, M. F.: Design of Machine Elements. Second ed., Prentice-Hall, Inc., 1953, pp. 441-447.
3. Oberg, Erik, and Jones, F. D.: Machinery's Handbook. Holbrook L. Horton, ed., 15th ed., The Industrial Press (New York), 1956, pp. 290-291.
4. Coulbert, C. D., MacInnes, W. F., Ishimoto, T., Bussell, B., and Ambrosio, A.: Temperature Response of Infinite Flat-Plates and Slabs to Heat Inputs of Short Duration at One Surface. Contract No. AF33(038)-14381, Univ. of California, Dept. Eng., Apr. 1951.
5. Hill, P. R.: A Method of Computing the Transient Temperature of Thick Walls From Arbitrary Variation of Adiabatic-Wall Temperature and Heat-Transfer Coefficient. NACA TN 1405, 1957.
6. Fay, J. A., and Riddell, F. R.: Theory of Stagnation Point Heat Transfer in Dissociated Air. Res. Rep. 1, AVCO Res. Lab., June 1956 (rev. Apr. 1957). (Formerly AVCO Res. Note 18.)
7. Maccoll, J. W., and Codd, J.: Theoretical Investigations of the Flow Around Various Bodies in the Sonic Region of Velocities. British Theoretical Res. Rep. No. 17/45, B.A.R.C. 45/19, Ministry of Supply, Armament Res. Dept., 1945.
8. Diaconis, N. S., Wisniewski, Richard J., and Jack, John R.: Heat Transfer and Boundary-Layer Transition on Two Blunt Bodies at Mach Number 3.12. NACA TN 4099, 1957.
9. Schlichting, H.: Lecture Series "Boundary Layer Theory." Part I - Laminar Flows. NACA TM 1217, 1949.

TABLE I
DESCRIPTION OF TEST MODELS

Model	Surface	Weight, g	Roughness, μ in., rms		Area increase, (percent)
			Measured (by mechanical methods)	Calculated (from photographs)	
1	Hemispherical pits	3.663	----	^a 13,700	13
2	Bidirectional grooves	3.202	----	^a 13,000	38.1
3	Unidirectional grooves	3.366	----	^a 13,000	32.2
4	Rough grind	3.600	^b 40	^c 70.2	10.0
5	Rough machine	3.716	^b 450	^c 1,035	30.9
6	Smooth machine	3.632	^b 45	^c 41.4	2.75
7	Smooth grind	3.465	^b 20	^c 28.3	7.0
8	As received	3.737	^b 12	^c 18.7	4.0
9	Polish	3.575	^d 15	^c 9.7	2.0
10	Mirror finish	3.618	^d 12	^c 8.00	1.0 ^a

^aCalculated from direct measurements and enlarged photographs.

^bMeasured with Physicists Research Co. Profilometer, Model No. 11, Type Q.

^cCalculated from measurements taken directly from photomicrographs of duplicate specimens.

^dMeasured with surface interferometer (Type L.C.A., No. 36) manufactured by La Précision Mécanique (Paris).

TABLE II
TUNNEL CONDITIONS FOR FLAT-FACE MODELS

Model	Stagnation temperature, °F	Chamber pressure, lb/sq in., gage	Mach number
1	3,510	90	2
2	3,510	90	2
3	3,550	90	2
4	3,500	90	2
5	3,520	90	2
6	3,540	90	2
7	3,520	90	2
8	3,520	90	2
9	3,520	90	2
10	3,560	90	2

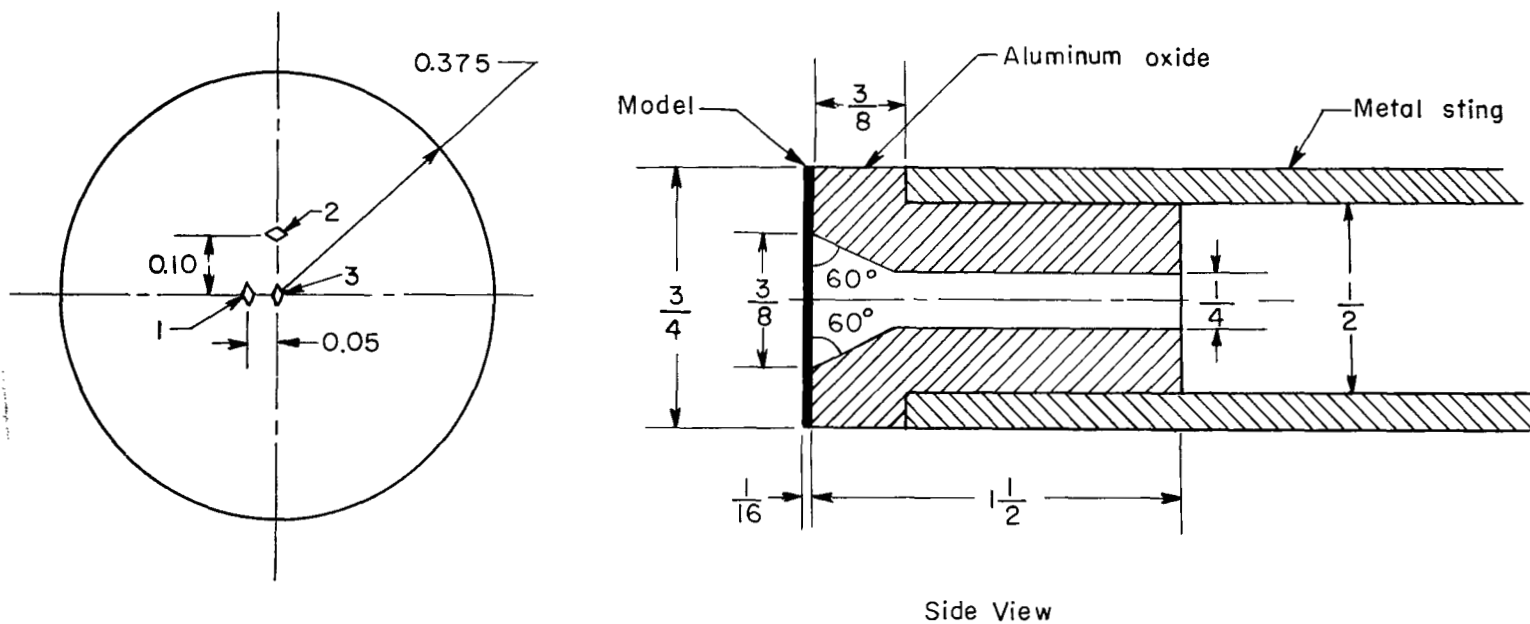
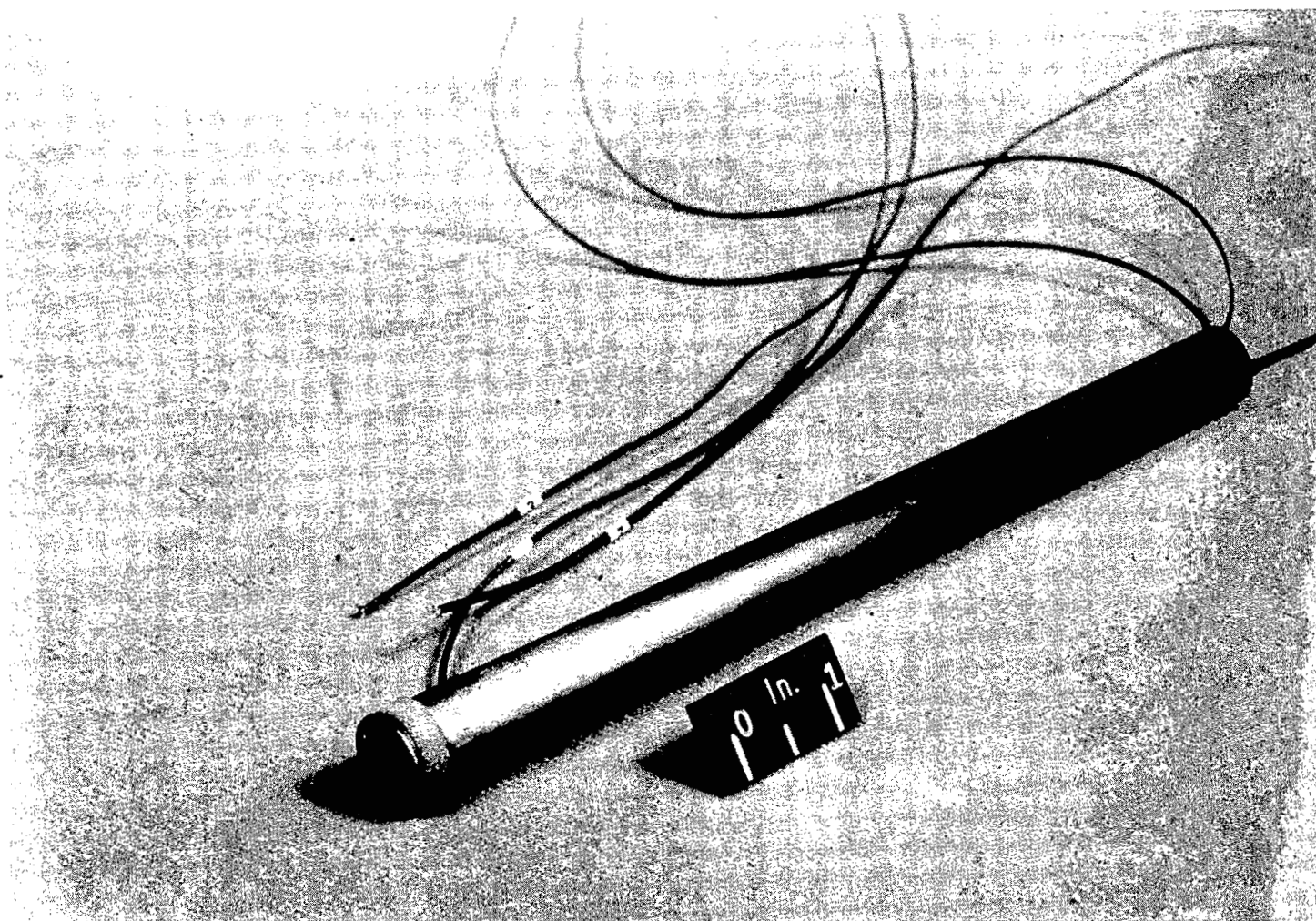


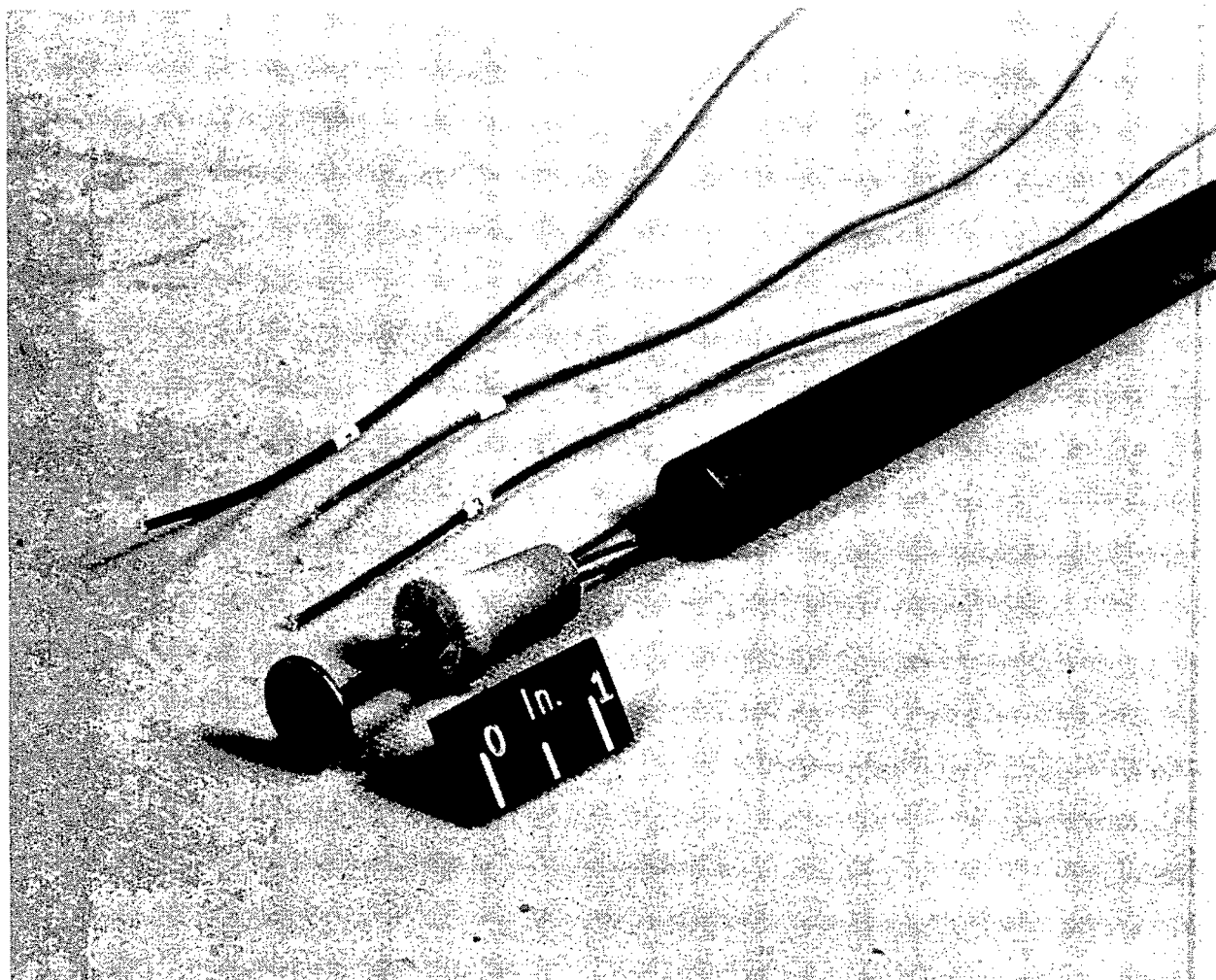
Figure 1.- Thermocouple locations for all models. All dimensions are in inches.



(a) Apparatus assembled for testing.

L-57-503

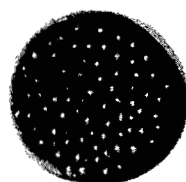
Figure 2.- Model assembly showing (left to right) model, aluminum oxide insulator, and sting.



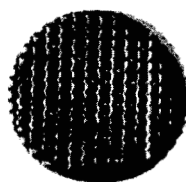
(b) Exploded view.

L-57-504

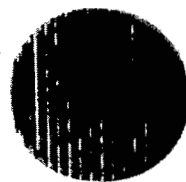
Figure 2.- Concluded.



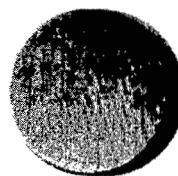
2



3



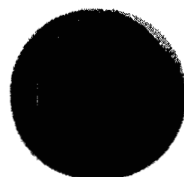
4



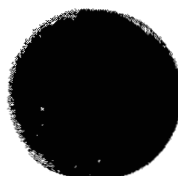
5



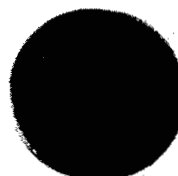
7



8



9



10

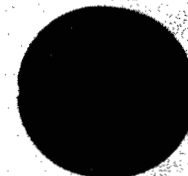


Figure 3.- Surfaces of models before testing. L-57-294

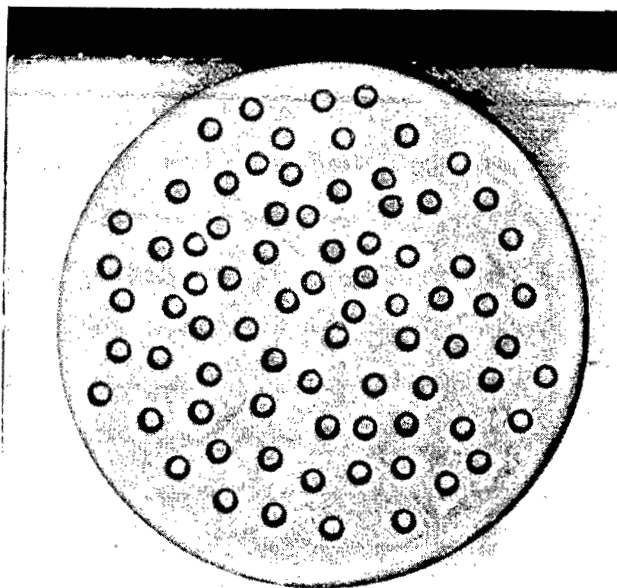


Figure 4.- Model 1 (hemispherical pits) before testing. L-57-291

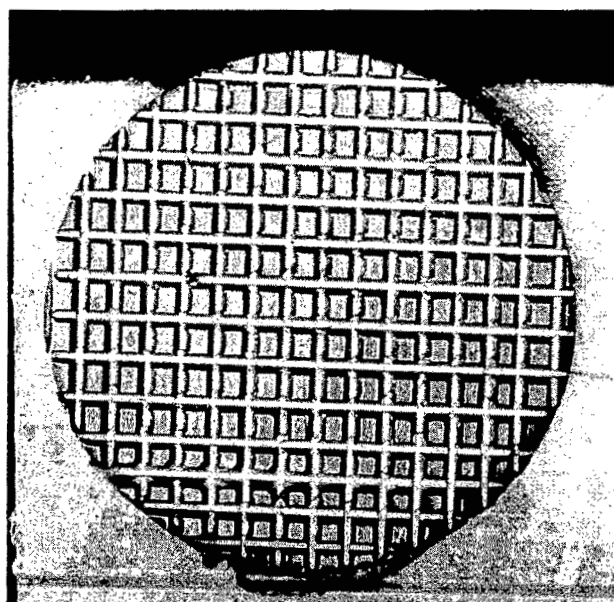


Figure 5.- Model 2 (bidirectional grooves) before testing. L-57-292

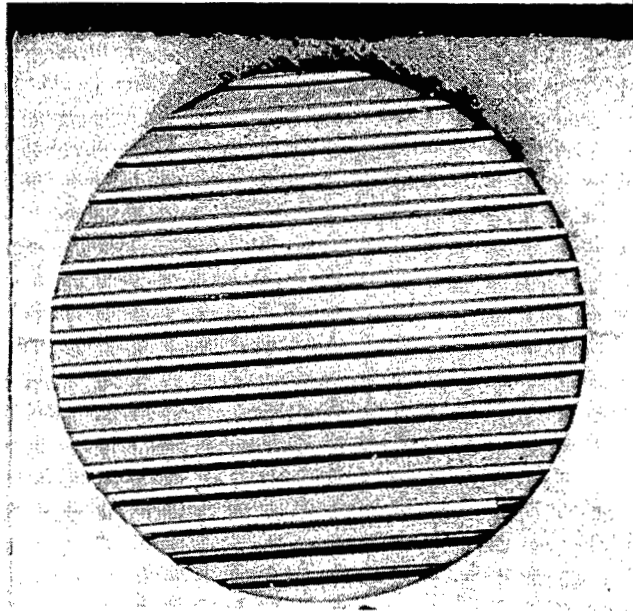


Figure 6.- Model 3 (unidirectional grooves) before testing. L-57-293

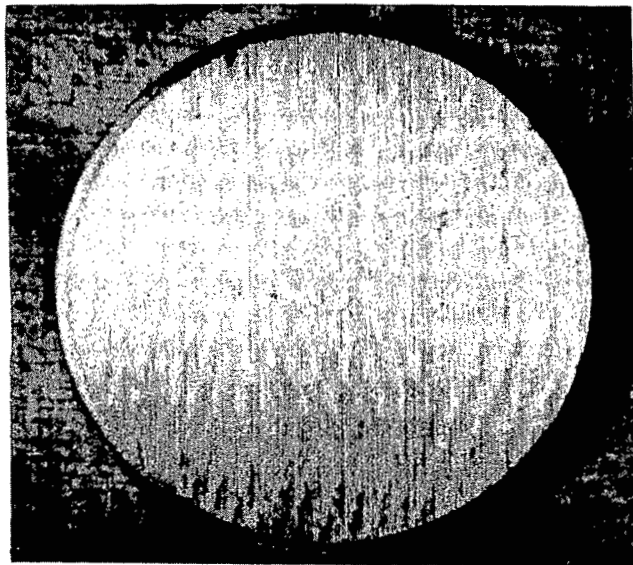


Figure 7.- Model 4 (rough grind) before testing. L-57-2195

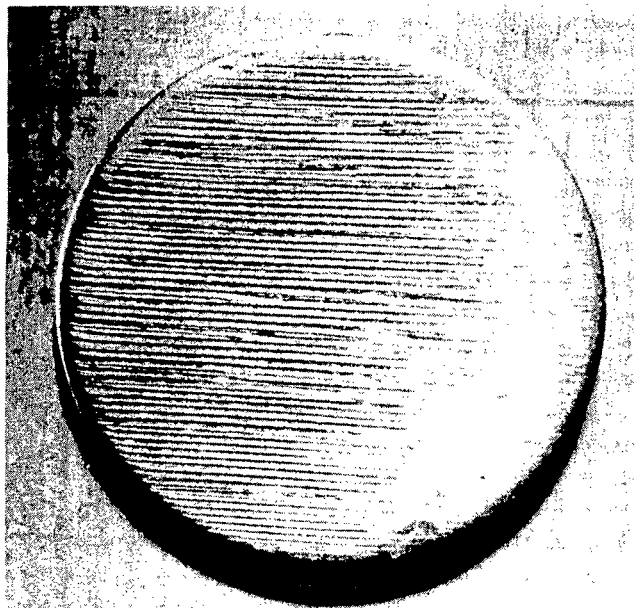


Figure 8.- Model 5 (rough machine) before testing. L-57-2194

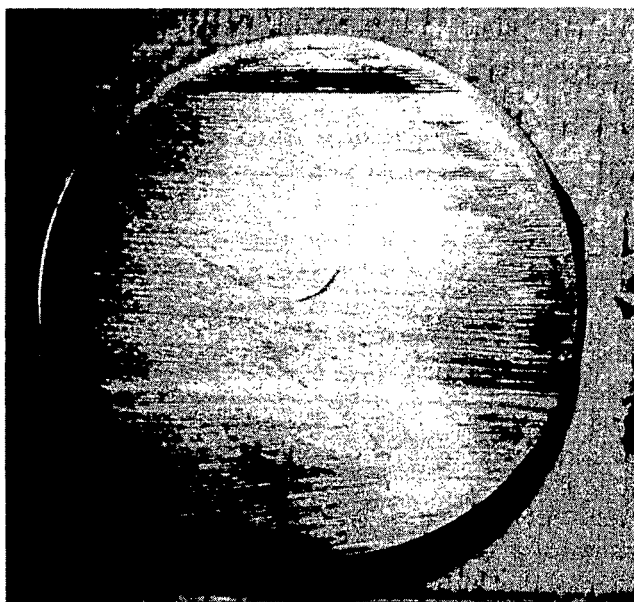
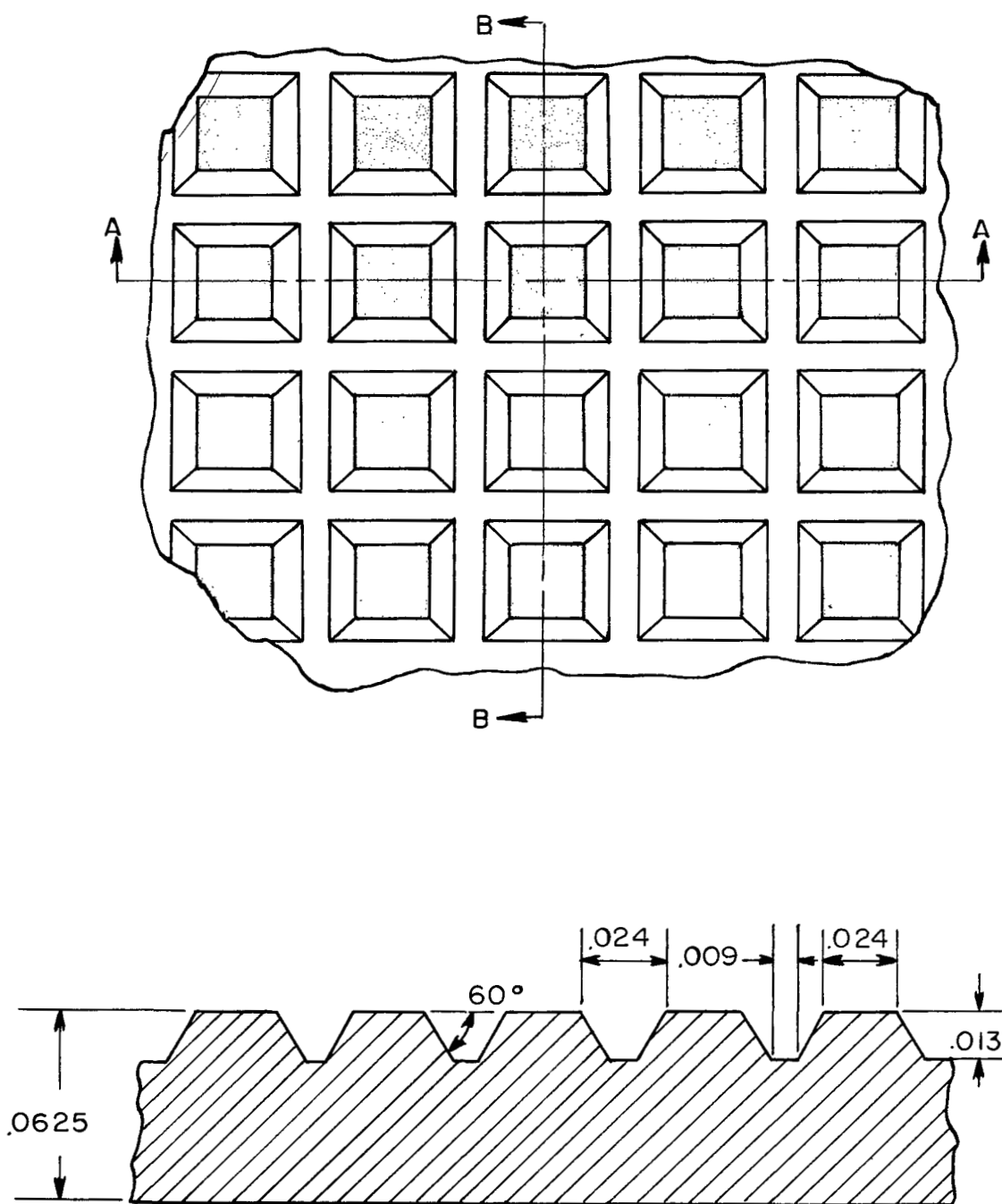
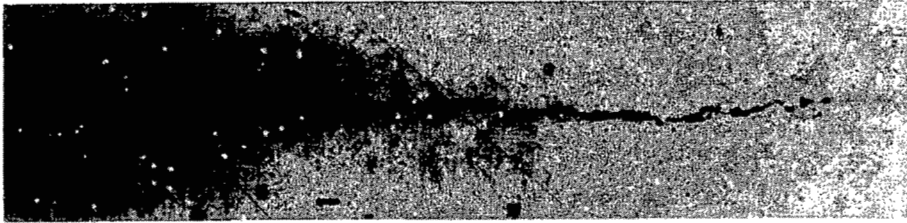


Figure 9.- Model 6 (smooth machine) before testing. L-57-2193

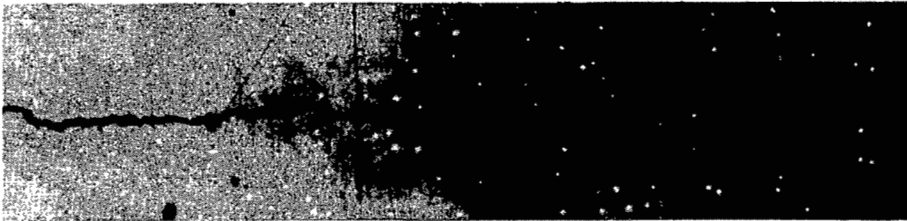


Sections A-A and B-B

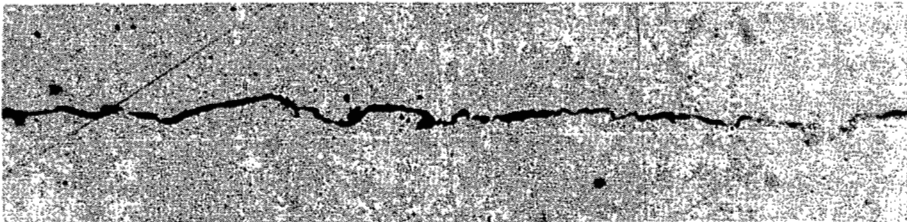
Figure 10.- Surface of model 2.



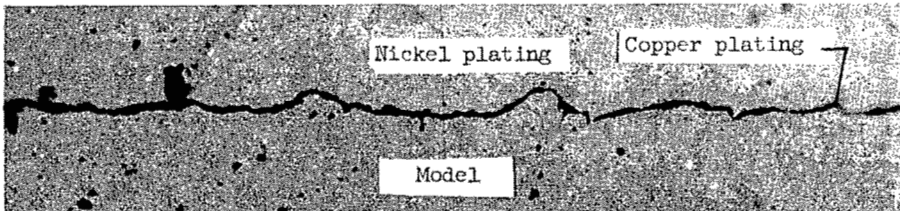
Sample 1

Calculated roughness, 84.94 $\mu\text{in. rms}$ 

Sample 2

Calculated roughness, 50.50 $\mu\text{in. rms}$ 

Sample 3

Calculated roughness, 77.49 $\mu\text{in. rms}$ 

Sample 4

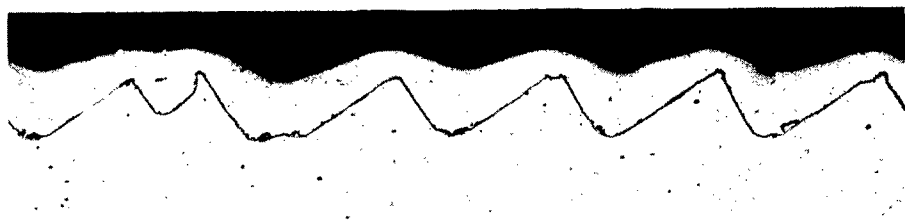
Calculated roughness, 67.90 $\mu\text{in. rms}$

—|—|—
0.001 in.

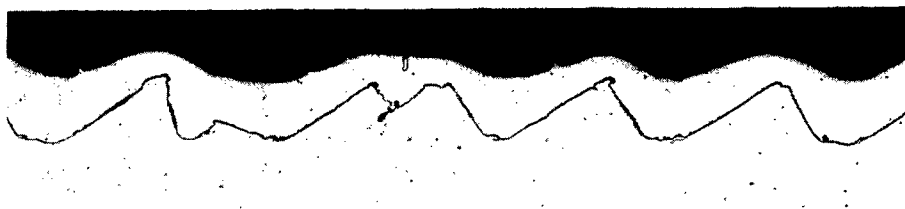
L-58-132

(a) Model 4 (rough grind).

Figure 12.- Photomicrographs of typical surface cross sections.



Sample 1

Calculated roughness, 1228. μ in. rms

Sample 2

Calculated roughness, 906. μ in. rms

Sample 3

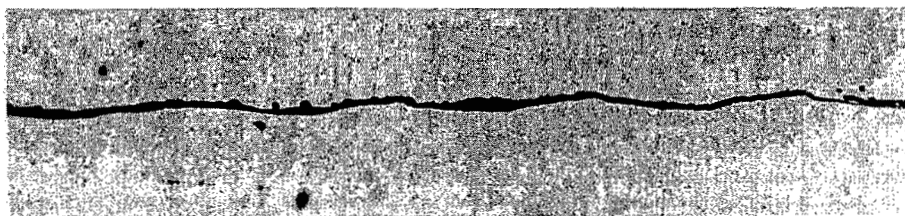
Calculated roughness, 971. μ in. rms

H
0.001 in.

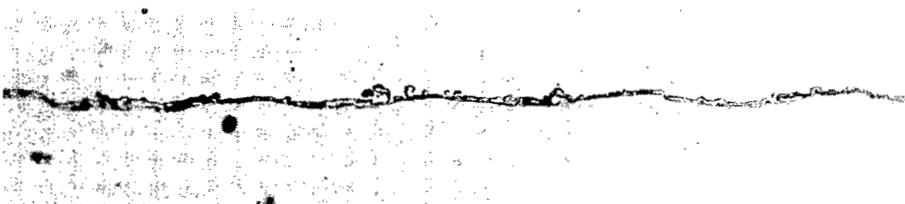
L-58-133

(b) Model 5 (rough machine).

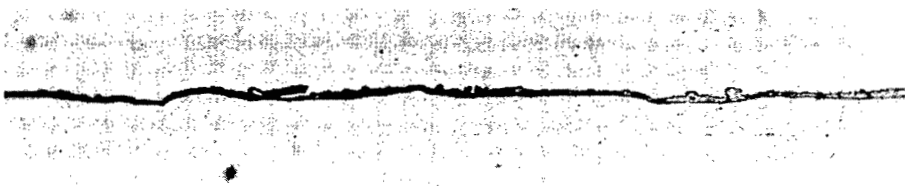
Figure 12.- Continued.



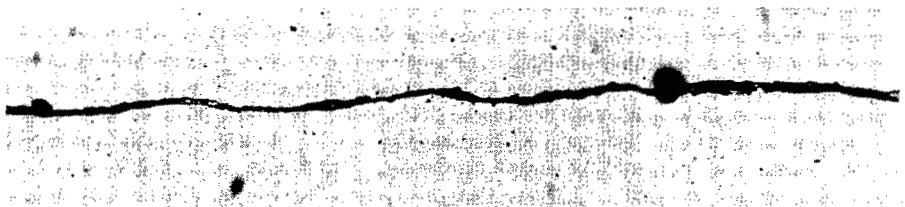
Sample 1

Calculated roughness, 36.29 $\mu\text{in. rms}$ 

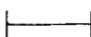
Sample 2

Calculated roughness, 14.71 $\mu\text{in. rms}$ 

Sample 3

Calculated roughness, 37.70 $\mu\text{in. rms}$ 

Sample 4

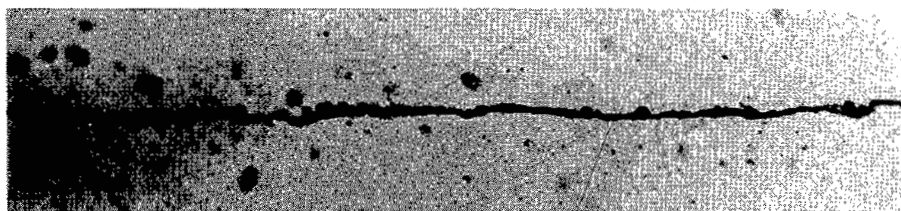
Calculated roughness, 44.91 $\mu\text{in. rms}$ 

0.001 in.

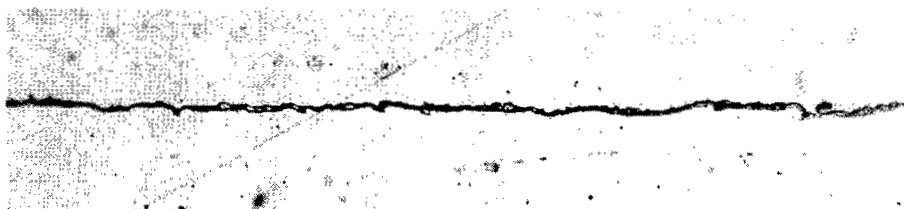
L-58-134

(c) Model 6 (smooth machine).

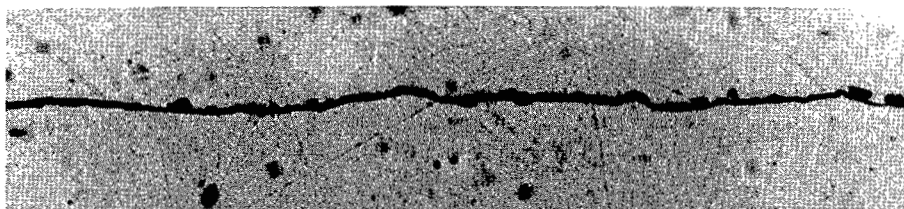
Figure 12.- Continued.




Sample 1

Calculated roughness, 30.30 $\mu\text{in. rms}$ 

Sample 2

Calculated roughness, 31.91 $\mu\text{in. rms}$ 

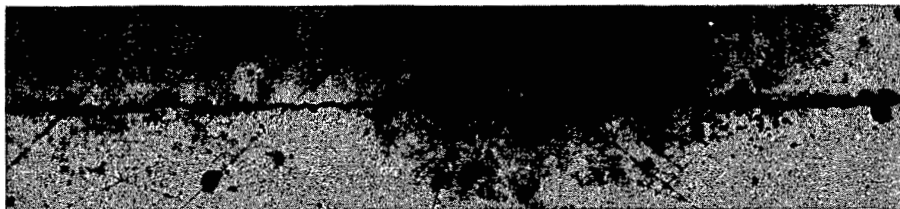
Sample 3

Calculated roughness, 22.56 $\mu\text{in. rms}$ 
0.001 in.

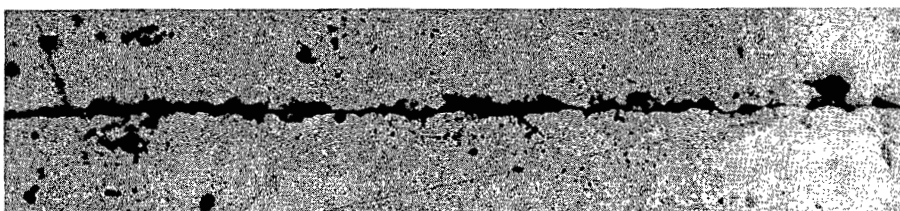
L-58-135

(d) Model 7 (smooth grind).

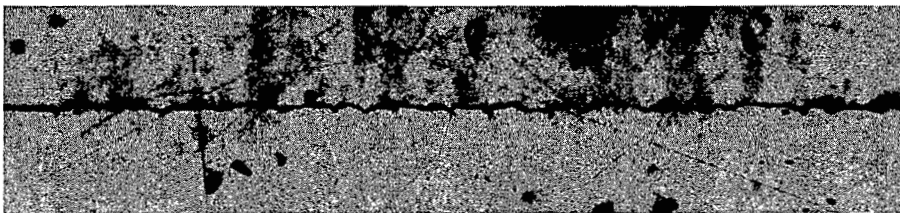
Figure 12.- Continued.



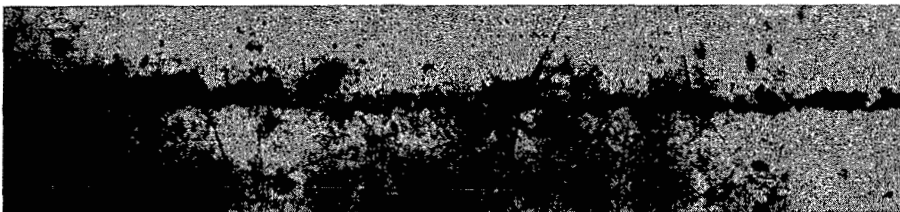
Sample 1

Calculated roughness, 22.09 μ in. rms


Sample 2

Calculated roughness, 7.28 μ in. rms

Sample 3

Calculated roughness, 18.36 μ in. rms

Sample 4

Calculated roughness, 26.96 μ in. rms

0.001 in.

L-58-136

(e) Model 8 (as received).

Figure 12.- Continued.



Sample 1

Calculated roughness, 9.50 μ in. rms



Sample 2

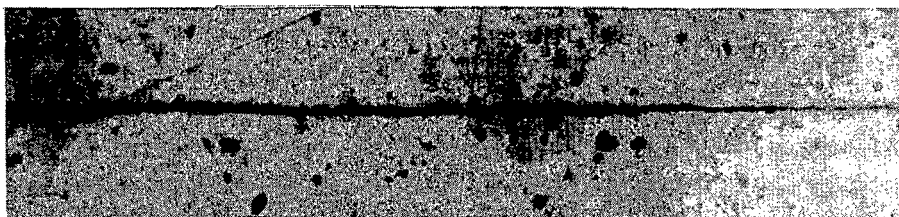
Calculated roughness, 9.70 μ in. rms

0.001 in.

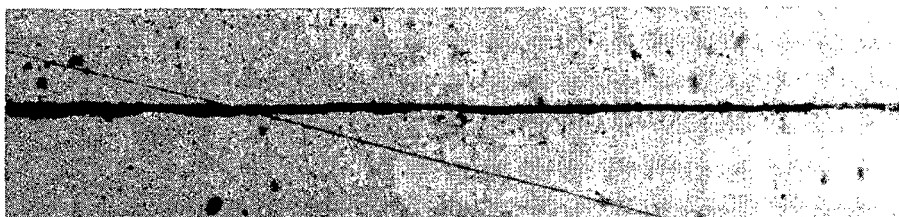
L-58-137

(f) Model 9 (polish).

Figure 12.- Continued.



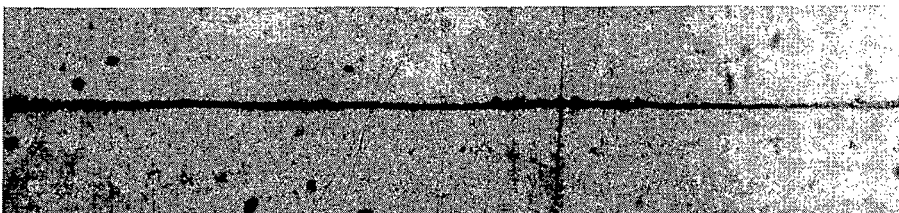
Sample 1

Calculated roughness, 10.44 $\mu\text{in. rms}$ 


Sample 2

Calculated roughness, 12.37 $\mu\text{in. rms}$ 

Sample 3

Calculated roughness, 7.00 $\mu\text{in. rms}$ 

Sample 4

Calculated roughness, 2.00 $\mu\text{in. rms}$ 

0.001 in.

L-58-138

(g) Model 10 (mirror finish).

Figure 12.- Concluded.

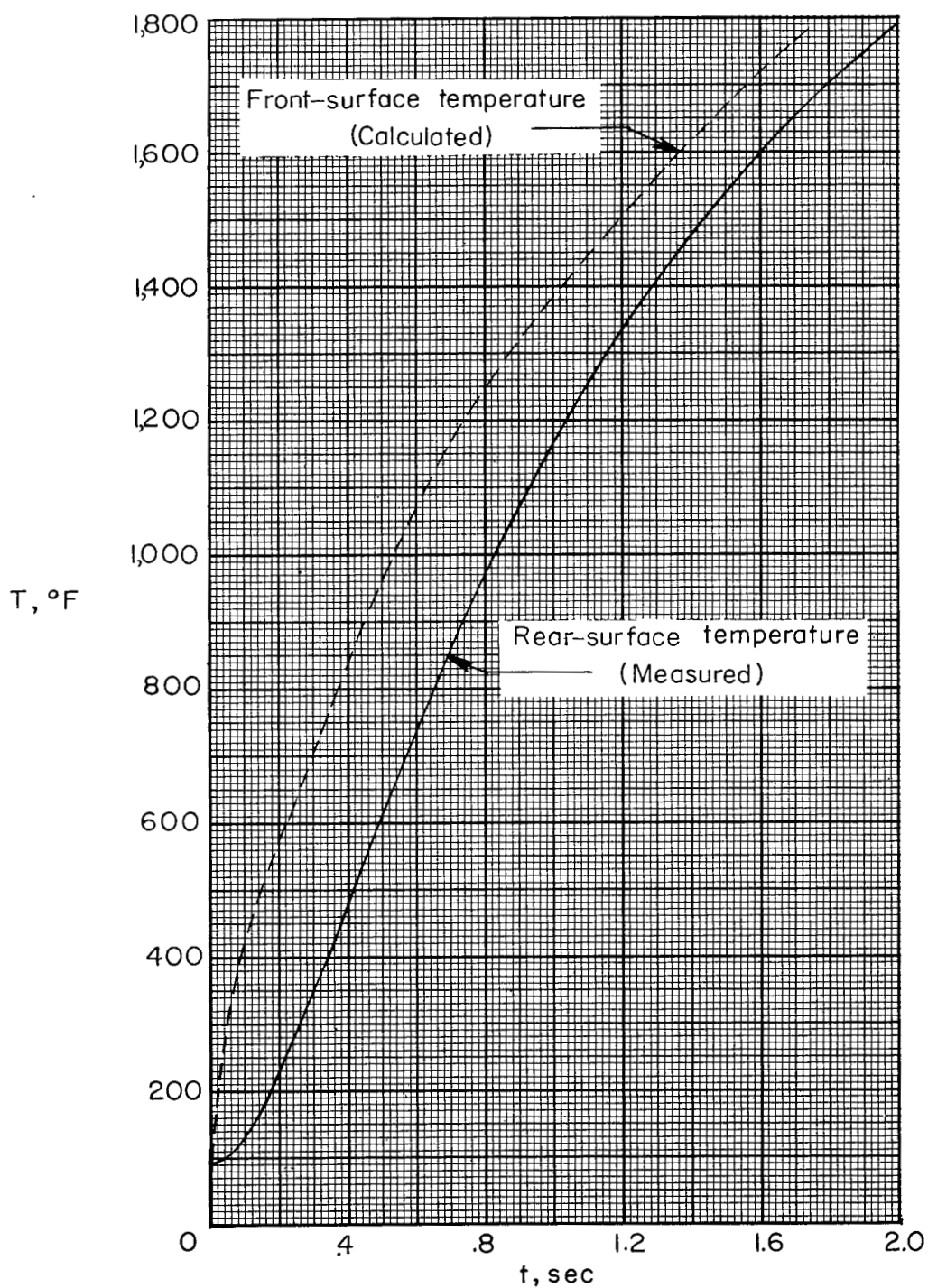


Figure 13.- Typical temperature time history of test models. Model 1, thermocouple 3.

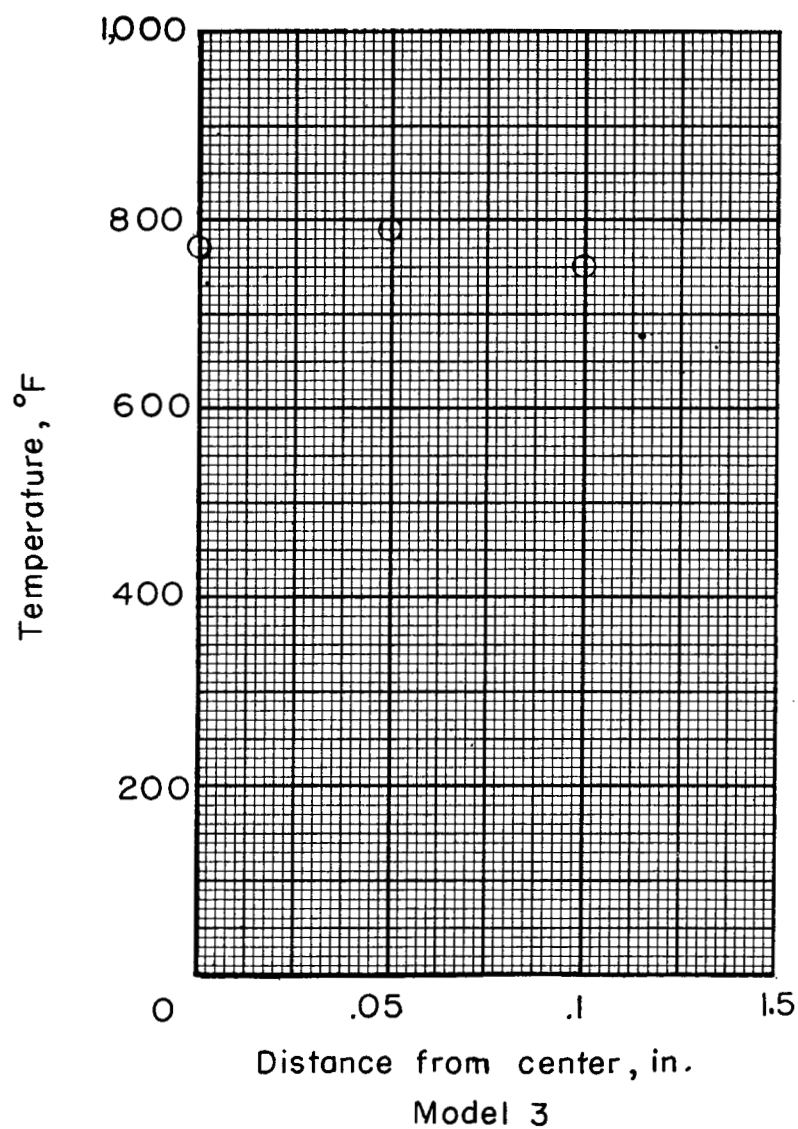
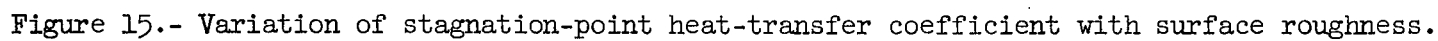


Figure 14.- Temperature gradient laterally across face of model;
 $t = 0.5$ second.



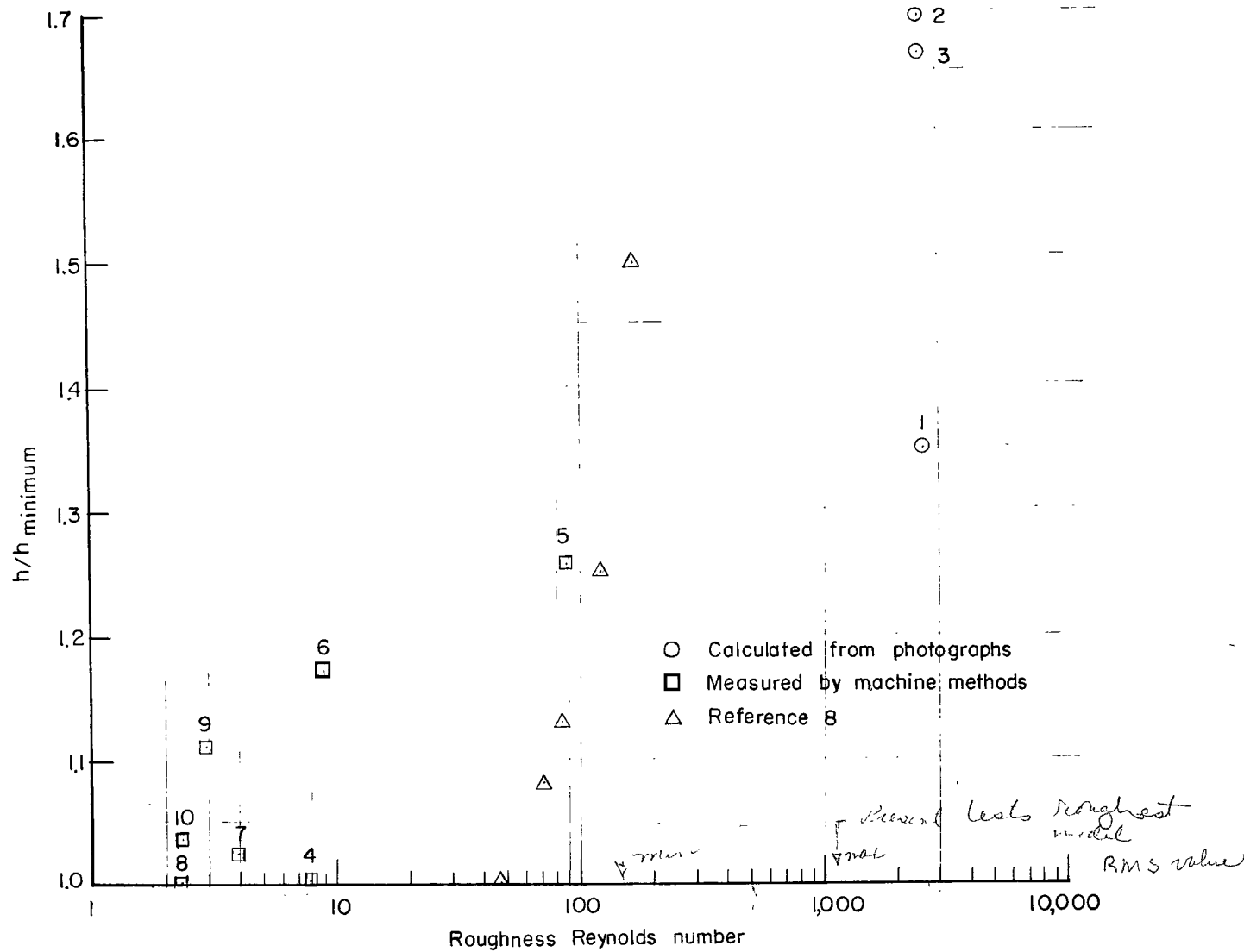


Figure 16.- Variation of heat-transfer coefficient with roughness Reynolds number.

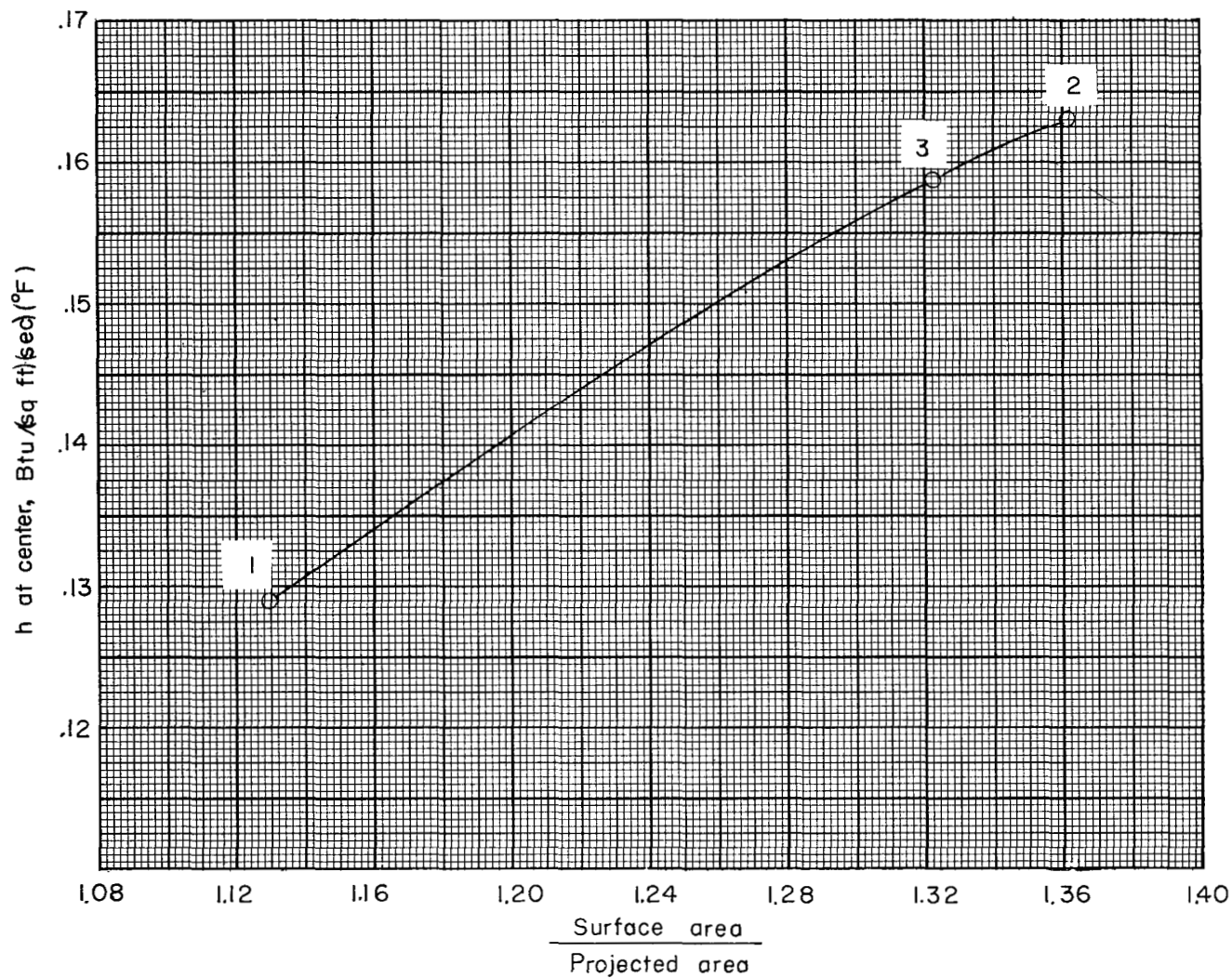


Figure 17.- Variation of heat-transfer coefficient with ratio of actual surface area to projected surface area for macroscopic roughnesses.



CONFIDENTIAL